Low-spin excitations in ^{97}Zr

T. Rząca-Urban, W. Urban, M. Czerwiński, and J. Wiśniewski
Faculty of Physics, University of Warsaw, ul. Pasteura 5, PL-02-093 Warszawa, Poland

A. Blanc, H. Faust, M. Jentschel, P. Mutti, U. Köster, and T. Soldner
Institut Laue-Langevin, F-38042 Grenoble, France

G. de France
Grand Accélérateur National d'Ions Lourds (GANIL), CEA/DSM - CNRS/IN2P3, Bd Henri Becquerel, BP 55027, F-14076 Caen Cedex 5, France

G. S. Simpson
LPSC, Université Grenoble Alpes, CNRS/IN2P3, Institut National Polytechnique de Grenoble, F-38026 Grenoble Cedex, France

C. A. Ur
Extreme Light Infrastructure-Nuclear Physics (ELI-NP)/IFIN-HH, 077125 Bucharest-Magurele, Romania

(Received 30 September 2018; published 13 December 2018)

The main goal of this work is the determination of spins and parities of excited states in ^{97}Zr, among others the 2264.3-keV level, which had previously been tentatively reported as the $11/2^-$ excitation corresponding to the $h_{11/2}$ neutron orbital. Low-spin excited states in ^{97}Zr were populated via the cold-neutron capture reaction. The γ rays emitted following the reaction were measured using the highly efficient array of high-purity germanium detectors, EXILL, at the Institut-Laue-Langevin (ILL), Grenoble. The primary γ rays deexciting the capture state in ^{97}Zr were identified for the first time. The new, precise neutron binding energy in ^{97}Zr of 5569.15(4) keV differs significantly from the value reported in the literature. The previously reported level scheme has been amended by several new low-spin levels. The (n, γ) data were complemented by a measurement of the β^- decay of ^{97}Y at the Lohengrin fission-fragment separator of the ILL, and the observation of the β^- decay of ^{97}Y populated in neutron-induced fission of ^{235}U and measured using the EXILL Ge array. The combined data allowed unique spin-parity assignments for many levels in ^{97}Zr. The 2264.3-keV level, with a new spin-parity assignment of $9/2^+$, may correspond to the $\nu g_{9/2}$ extruder orbital.

DOI: 10.1103/PhysRevC.98.064315

I. INTRODUCTION

The $^{97}_{40}Zr_{57}$ isotope is located at the border of the $A = 100$ region of highly deformed nuclei, where a sudden onset of deformation in Sr and Zr isotopes is observed around the neutron number $N = 59$. Isotopes with $N < 59$ are spherical in their ground state due to the $d_{5/2}$ and $s_{1/2}$ neutron shell closures at $N = 56$ and $N = 58$, respectively. This sphericity is further enhanced at $Z = 40$ (Zr) by the $p_{1/2}$ proton shell closure.

It has been proposed that the onset of deformation in this region is primarily due to the occupation of the deformation-driving, low-Ω orbitals originating from the $h_{11/2}$ neutron shell [1–3], helped by vacating the $9/2^+[404]$ neutron extruder [4]. This proposition has been recently challenged by a claim that the deformation sets in due to a massive excitation of protons to the $g_{9/2}$ orbital, called "type II shell evolution," where the $9/2^+[404]$ neutron extruder does not play any role [5].

Because of subshell closures in ^{96}Zr and ^{98}Zr the ground and excited levels in ^{97}Zr can be seen as a coupling of a neutron particle or hole to even-even neighbors. The promotion to the $g_{9/2}$ proton and the $g_{7/2}$ and $h_{11/2}$ neutron orbitals, which are unoccupied, will form excited levels in ^{97}Zr. The observation of such levels helps determine single-particle energies. The knowledge on this subject is still not satisfactory, especially concerning the $h_{11/2}$ neutron, which was proposed as the dominating component of the $11/2^-$ excitation (2263.7 keV) in ^{97}Zr [6]. This level has some unusual properties. Its main decay branch is an $M2$ transition with an enormous strength of 0.52 W.u. [7]. To support this multipolarity, an analogous 522-keV decay of the 831-keV $11/2^-$ isomer in ^{97}Sr with 0.7 W.u. was quoted in Ref. [6]. However, as was shown later [8,9], this isomer in ^{97}Sr corresponds to the $9/2^+[404]$ extruder. The only $11/2^-$ level in the vicinity is the 0.76 μs isomer at 684.1-keV in ^{99}Mo, which besides a much lower excitation energy has also lower rate of 0.1 W.u. of its 448.6-keV, M2 decay [10].

In this work we complement the data on ^{97}Zr [7] with new information obtained from the cold-neutron capture reaction, often considered to be a "complete spectroscopy" for

low-spin excitations. The cold-neutron capture on the 0^+ ground state of ^{96}Zr has the advantage of the known, $1/2^+$ spin-parity of the capture level in ^{97}Zr. Observing intensities of γ decays from this level (primary transitions) often allows one to conclude about spins of levels they populate. It is worth noting that neutron capture may populate levels which are not populated in β decay or other reactions. Due to a complex structure of the capture level, its decays may populate collective excitations, in contrast to the population in β decay, which often favors transitions to levels with dominating single-particle components. In this way the neutron capture may help in tracing the collectivity emerging in ^{97}Zr.

In addition to the neutron capture measurement, we have revised previous results from the β^- decay of the $1/2^-$ and $9/2^-$ isomers of ^{97}Y [6]. The purpose of this study was to verify decay branchings, which may help spin-parity assignments. In addition, our experiment allowed to search for new isomeric levels in a range from micro- to milliseconds.

We also used data from the cold-neutron-induced fission of ^{235}U, containing high-statistics data on the β^- decay of ^{97}Y, to analyze angular correlations and directional-polarization correlations for γ-γ cascades in ^{97}Zr.

In Sec.II of the paper we describe briefly experimental setups and data analysis techniques. Section III presents experimental results and the new level scheme of ^{97}Zr. In Sec.IV we discuss the properties of ^{97}Zr. Concluding remarks are collected in Sec.V.

II. EXPERIMENTS AND ANALYSIS TECHNIQUES

A. Cold-neutron capture measurement

Until now there was no report on slow (cold or thermal) neutron capture on a ^{96}Zr target, probably because of the very low neutron-capture cross section of ^{96}Zr, which is 0.02 b, only. The present work reports the first measurement of cold-neutron capture on a ^{96}Zr target. The progress was possible due to the use of the very efficient EXILL array [11].

The experiment was performed at the PF1B cold-neutron beam facility of the Institut-Laue-Langevin (ILL), Grenoble. To measure γ rays from the neutron-capture reaction we used the EXILL array consisting of 16 high-purity germanium (HPGe) detectors: 8 EXOGAM clover detectors [12], 6 GASP [13] detectors with bismuth germanate (BGO) anti-Compton shields, and two clovers from the Lohengrin instrument of ILL. Such a highly efficient HPGe array was used for the first time in neutron capture studies. Precise energy and efficiency calibrations of EXILL were performed in the energy range from 30 keV to 10 MeV, using standard calibration sources of ^{133}Ba, ^{60}Co, and ^{152}Eu as well as data from the reactions ^{27}Al$(n,\gamma)^{28}$Al and ^{35}Cl$(n,\gamma)^{36}$Cl. More information on the EXILL array, the neutron beam, the collimation system, the data acquisition system, the target chamber, and analysis techniques can be found in Refs. [11,14].

The high efficiency of EXILL allowed collection of about 3.3×10^{10} triggerless events in a 21 hour measurement. In Figs. 1 and 2 we show singles γ spectra from the cold-neutron capture on the Zr target, measured in this work. The isotopic composition of the Zr target is given in Table I. However, the

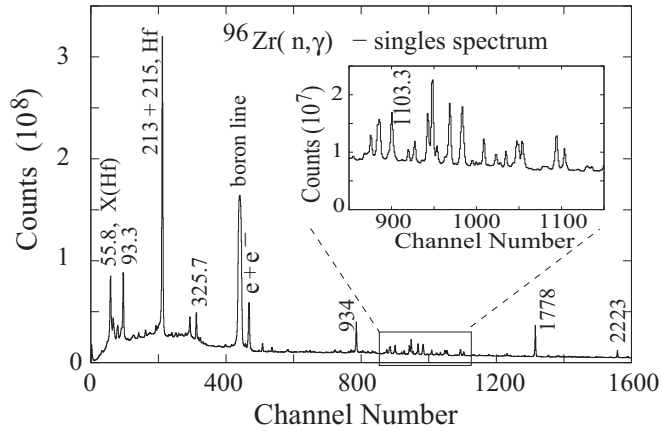

FIG. 1. Low-energy part of the γ singles spectrum from the ^{96}Zr$(n,\gamma)^{97}$Zr reaction, measured in this work. Lines are labeled with γ energies in keV. The inset shows part of the spectrum with the strongest, 1103.3-keV line from ^{97}Zr. Constant-peak-width calibration is applied; see the text for more explanation.

target sample contained also impurities of Hf isotopes (about 0.3%) and traces of boron. Due to their significantly higher neutron capture cross-sections (104 and 760 b respectively) the corresponding lines are clearly visible in the spectrum. The powder was contained in two sealed FEF (fluorinated ethylene propylene copolymer) bags with 25 μm thick layers each. Captures on FEP (carbon and fluorine) are negligible (<1% of total capture rate).

The low-energy part of the spectrum is dominated by γ lines of ^{178}Hf and ^{180}Hf [15–17]. Also visible are the 934-keV line of ^{92}Zr, the strong, Doppler broadened 478-keV line due to ^{10}B$(n,\alpha\gamma)$ reactions, and lines of ^{2}H (2223 keV) and ^{28}Al (1779, 7724 keV) from the capture in the surrounding materials of neutrons scattered on the massive target. Insets in both figures show lines of ^{97}Zr, corresponding to the 1103.3-keV ground-state transition and the 4465.8-keV primary

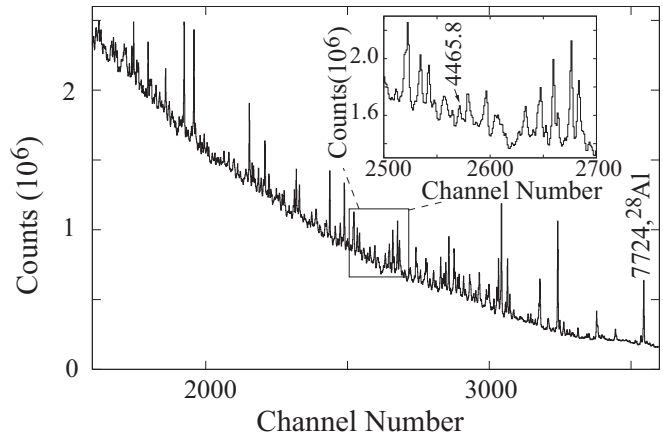

FIG. 2. High-energy part of the γ singles spectrum from the ^{96}Zr$(n,\gamma)^{97}$Zr reaction, measured in this work. Lines are labeled with γ energies in keV. The inset shows part of the spectrum with the strongest, 4465.8-keV primary line from ^{97}Zr. Constant-peak-width calibration is applied.

TABLE I. The isotopic composition of the Zr target used in this work.

^{90}Zr	^{91}Zr	^{92}Zr	^{94}Zr	^{96}Zr
19.3%	5.1%	7.8%	8.2%	59.6%

decay to the 1103.3-keV transition is contaminated by lines of hafnium.

The ^{28}Al lines were used for an internal energy calibration, because of their very precisely known energies [18]. In order to optimize the analyzed histograms energy range up to 8 MeV we applied the so-called constant-peak-width energy calibration. This is a strongly nonlinear calibration, $E_\gamma = C_0 + C_1 \times (\text{channel}) + C_2 \times (\text{channel})^2$, where $C_0 = -0.18$ keV, $C_1 = 0.950573$ keV/channel, and $C_2 = 0.000306016$ keV/channel^2. With this calibration (nonlinear compression) the peak width is approximately constant over the whole energy range, enhancing the visibility of high-energy γ lines without losing the resolving power.

To extract the information on ^{97}Zr nuclei we used various two- and three-dimensional histograms sorted out of multiple-γ coincidences, created from triggerless events by applying a 200 ns time window. Particularly useful was the so-called $gS2$ histogram, where on the g axis we sorted two γ energies of a coincidence event while on the S axis we sorted their sum. The energy of the neutron-capture state is a well defined, characteristic signature of a nucleus. Therefore, gating on such energy on the S axis produces a clean spectrum containing lines in cascades belonging to this nucleus.

In Fig. 3 we show the total projection on the S axis of the $gS2$ histogram. In the inset the gate on the 5569-keV line, corresponding to the neutron-capture energy in ^{97}Zr, is marked. In Fig. 4 a γ spectrum gated on the 5569-keV line in the total projection of the $gS2$ histogram is shown. The

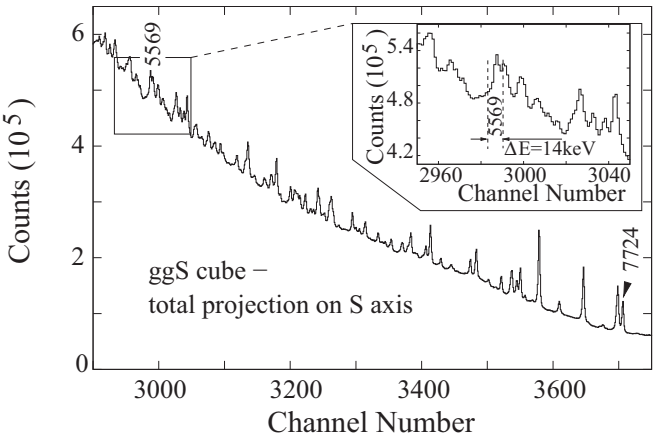

FIG. 3. Spectrum of summed energies of γ rays in twofold cascades depopulating the capture state in ^{97}Zr nucleus, following the ^{96}Zr + n reaction. Lines are labeled with γ energies in keV. The inset shows part of the spectrum with the 5569-keV line corresponding to neutron binding energy of ^{97}Zr, determined in this work. Constant-peak-width calibration is applied.

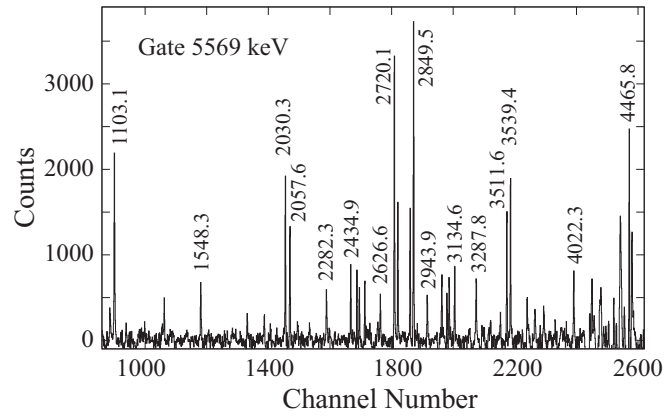

FIG. 4. γ rays in two-fold cascades depopulating the capture state in ^{97}Zr nucleus, following the ^{96}Zr + n reaction. The spectrum is gated on the 5569-keV line in the $gS2$ histogram. Lines are labeled with their γ energies in keV. Constant-peak-width calibration is applied.

spectrum contains pairs of γ lines with energies summing up to 5569 keV. One can see here the 1103.1- and 4465.8-keV pair of lines belonging to ^{97}Zr. Because at 5569 keV the width of the line and the width of the corresponding gate is about 14 keV, the spectrum in Fig. 4 contains also some contaminating pairs of γ lines from Hf isotopes, for which their sum fits the range (5569 ± 7) keV. We used further $\gamma\gamma$ and $\gamma\gamma\gamma$ histograms to assign lines seen in Fig. 4 to particular isotopes.

Figure 5 shows a gate on the 7724-keV line in the total projection on the S axis of the $gS2$ two-dimensional histogram. The 7724-keV line corresponds to the neutron binding energy of ^{28}Al, present in our data, which is produced in the ^{27}Al$(n\gamma)$ reaction by neutrons scattered from the target, hitting aluminum the elements of our experimental setup. In Fig. 5, well known lines in major twofold cascades in

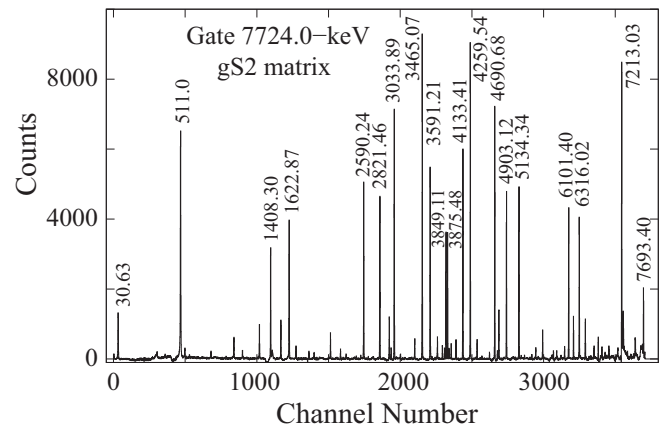

FIG. 5. γ rays in twofold cascades depopulating the capture state in ^{28}Al nucleus, following the ^{27}Al + n reaction. The spectrum is gated on the 7724.0-keV line in the $gS2$ matrix. Lines are labeled with their γ energies in keV. See text for more explanation. Constant-peak-width calibration is applied.

^{28}Al [18] can be seen. Again, the very clean spectrum and low background, specific for this type of analysis, proves its usefulness.

Despite the low statistics of the data corresponding to ^{97}Zr, it was also possible to extract useful information on angular correlations for γ-γ cascades connecting the capture level and the ground state. This is because both states have known $1/2^+$ spin-parity and the $1/2 \rightarrow 5/2 \rightarrow 1/2$ and $1/2 \rightarrow 3/2 \rightarrow 1/2$ cascades have very large but distinctly different angular-correlation anisotropies, while the $1/2 \rightarrow 1/2 \rightarrow 1/2$ cascade is isotropic.

B. Measurement of β decay of the $A = 97$ isobars at Lohengrin

To search for possible new isomers in ^{97}Zr, we performed a measurement at the Lohengrin fission-fragment separator [19] of ILL Grenoble. We measured γ rays from mass $A = 97$ ions, arriving at the detection point about 1.7 μs after being produced in fission of ^{235}U induced by thermal neutrons inside the ILL reactor. The measurement provided also good γ-coincidence data for verifying and extending the existing information on β decay of the ground state and the $9/2^+$ isomer in ^{97}Y.

The detection setup consisted of an ion chamber and three Ge detectors: two clover and a GammaX detector. In the measurement we used an electrostatic deflection system of Lohengrin, operating at the frequency of 100 Hz, chosen to search for isomers in the millisecond range. The precise time signals from the ion chamber and the use of digital electronics with 40 MHz clock provided also the possibility to measure half-lives in a range from 0.5 to 50 μs. The ions collected at the detection point were not transported away. For more details about this technique see Refs. [9,20].

In the measurement about 2.4×10^8 triggerless events were collected, comprising signals from Ge detectors and the ion chamber. These events were arranged into coincidence events using various time windows (200, 300, and 600 ns) and sorted into two- and three-dimensional histograms for further analysis.

Figure 6 illustrates the quality of our time measurement showing the time-delayed spectrum from the decay of the known 830.2-keV isomer in ^{97}Sr [9], interpreted as due to the $\nu 9/2^+[404]$ extruder. Time is counted from the registration of an ion by the ion chamber to the registration of a γ signal in a Ge detector. The spectrum is gated on the 522.1-keV line from the isomeric decay. The half-life extracted from this spectrum is 504(8) ns. Such a short half-life is not visibly influenced by the random start-stop effect present in this type of measurements (see Fig. 16 in Ref. [20]). The new value is in good agreement with the previously reported values of 526(13) ns [9] and 515(10)ns [21]. We note that the compilation [7] reports a 395(132) ns half-life for this level. The large, unsatisfactory uncertainty is a compromise between distinctly different values of about 260 and 500 ns [7]. In our opinion the value around 500 ns is the correct one.

The correctness of the present measurement is supported by the analysis of the well known 5.3(3) μs isomer at 270.1(2) keV in ^{88}Br [22], decaying by the 111.0(1)–159.1(1)-keV cascade, as shown in Fig. 7. The isomer, which at an

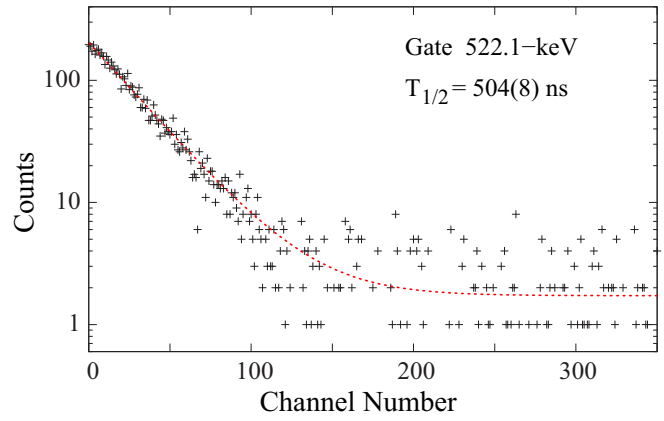

FIG. 6. Time-delayed spectrum gated on the 522.1-keV isomeric transition in ^{97}Sr, as observed in the present Lohengrin measurement. The red line represents the (exponent + constant background) fit to the data. Time calibration is 25 ns/channel.

$A/q = 5.5$ setting of the Lohengrin separator is separated as ^{88}Br^{16+} jointly with ^{99}Y^{18+}, is seen well in our measurement. The fit to the spectrum gives a half-life of 5.5(1) μs, in good agreement with the literature [22]. The statistical uncertainty is 0.04 μs, but because we applied a 2.0% correction connected with the random start-stop for this type of measurement [20], the total uncertainty was increased to 0.1 μs.

The quality of the γ data is illustrated in Figs. 8 and 9. Figure 8 displays, on a logarithmic scale, the total projection of the $\gamma\gamma$ histogram of coincidences sorted out of the data collected with Lohengrin. Figure 9 shows a γ spectrum gated on the 1400.3-keV line of ^{97}Zr.

C. Precise angular correlations and linear polarization with EXILL

We used the data from the measurement of neutron-induced fission of ^{235}U, collected during the EXILL campaign at the PF1b cold-neutron facility of ILL Grenoble [11]

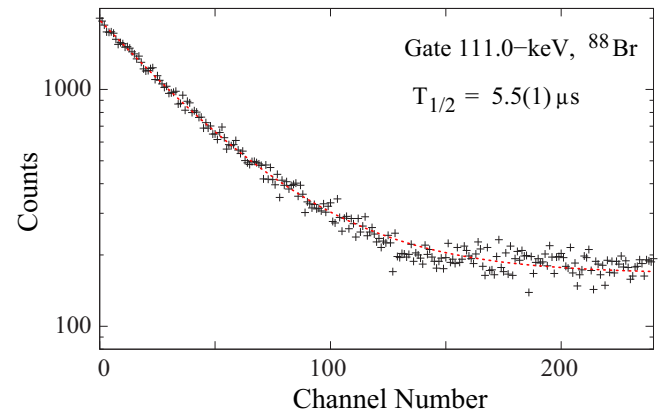

FIG. 7. Time-delayed spectrum gated on the 111.0-keV isomeric transition in ^{88}Br, as observed in the present Lohengrin measurement. The red line represents the (exponent + constant background) fit to the data. Time calibration is 200 ns/channel.

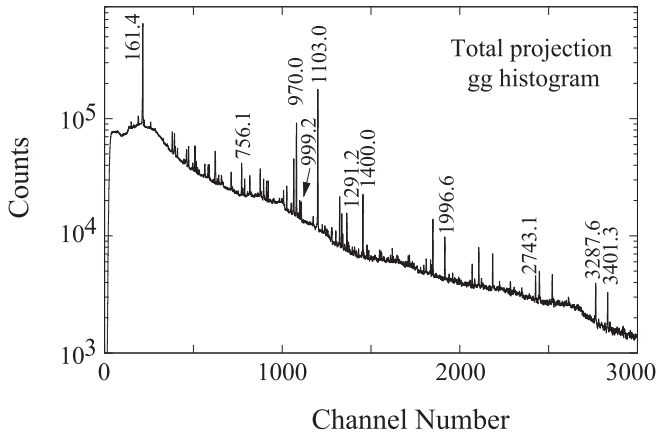

FIG. 8. Total projection of the $\gamma\gamma$ histogram of coincidences from β^- decay of $A = 97$ isobars, collected at Lohengrin. Major lines of ^{97}Zr are labeled with their γ energies in keV.

(EXILL-fission data). High cumulative yield of ^{97}Y in this reaction provided data to study its β decay to ^{97}Zr. Although not as clean as from Lohengrin, these data have high statistics, and can be used for precise correlation measurements possible with EXILL [11].

To determine spins and parities of excited states in ^{97}Zr we have analyzed γ-γ angular correlations. We used eight clover detectors mounted in one plane in an octagonal geometry. This configuration provides three different angles between detector pairs, 0°, 45°, and 90°. In the analysis we used formulas and conventions of Refs. [23,24]. The angular correlation function between two consecutive γ transitions in a cascade from a nonoriented state is expressed as a series of Legendre polynomials P_k,

$$W(\theta) = \sum_k A_k P_k(\cos\theta). \quad (1)$$

where θ is the angle between the directions of the γ_1 and γ_2 transitions in the cascade. The experimental A_k/A_0

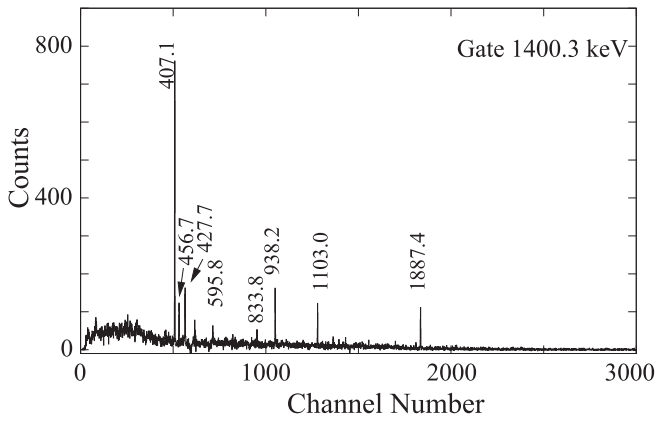

FIG. 9. γ spectrum gated on the 1400.3-keV line in the $\gamma\gamma$ histogram of coincidences from β^- decay of $A = 97$ isobars, collected at Lohengrin. Major lines of ^{97}Zr are labeled with their γ energies in keV.

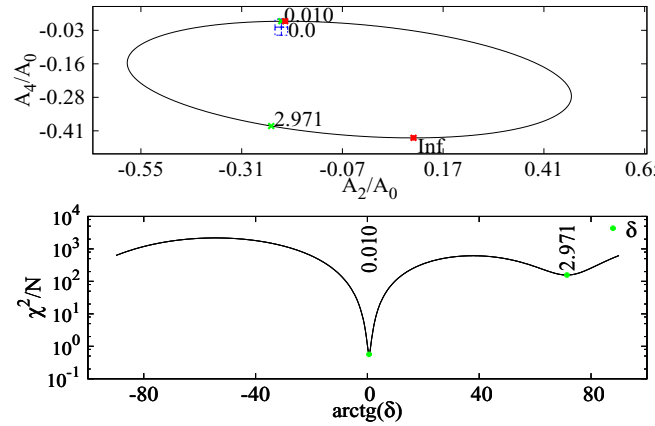

FIG. 10. Angular correlations for the 3/2-5/2-1/2 spin hypothesis in the 1291.1–1996.6-keV cascade as observed in the EXILL fission measurement. See text for more explanations.

coefficients were compared to theoretical values of A_k coefficients calculated for various hypotheses of spins, multipolarities, and mixing coefficients δ to find the best solutions. Further information on the technique, formulas, and examples of the analysis can be found in Refs. [14,25,26].

Figure 10 illustrates the quality of the angular-correlation measurement for the 3/2-5/2-1/2 spin hypothesis in the 1291.1–1996.6-keV cascade in ^{97}Zr with the unique solution at $\delta(1291.1) = 0.010(16)$. The ellipse in the upper panel of the figure represents theoretical values of A_2/A_0 and A_4/A_0 coefficients for the assumed spin hypothesis as a function of the mixing ratio δ_1 of the 1291.1-keV transition, varying from 0 to $\pm\infty$ (red dots) along the two branches of the ellipse. Here the 1996.6-keV transition is assumed to be an unmixed, stretched quadrupole with $\delta_2 = 0$. The experimental values of A_2/A_0 and A_4/A_0 with their error bars are represented by the blue rectangle. The lower panel of the figure shows a plot of the corresponding function of χ^2 per degree of freedom.

For strong transitions in ^{97}Zr we could also determine linear polarization by measuring directional-linear-polarization correlations in $\gamma\gamma$ cascades, using EXOGAM clover detectors as Compton polarimeters. More information on the technique of directional-linear-polarization correlations and new formulas derived for such an analysis can be found in Ref. [26].

III. DATA ANALYSIS AND EXPERIMENTAL RESULTS

A. Level scheme of ^{97}Zr

Prior to this work low- and medium-spin levels in ^{97}Zr were observed following the β^- decay of ^{97}Y [6,27] and in (d, p) and $(\alpha, ^3\text{He})$ direct reactions [28]. The yrast structure was also studied up to spin $33/2^+$ using heavy-ion induced fission reactions induced by ^{48}Ca on a thick ^{238}U target [29].

We searched for new levels and transitions in ^{97}Zr using the data from the (n, γ) reaction on ^{96}Zr, measured with EXILL, and from the β decay of ^{97}Y measured at Lohengrin.

1. Results from ^{96}Zr$(n, \gamma)^{97}$Zr reaction

New lines were searched for in γ spectra obtained by gating on the already known lines, using various double- and

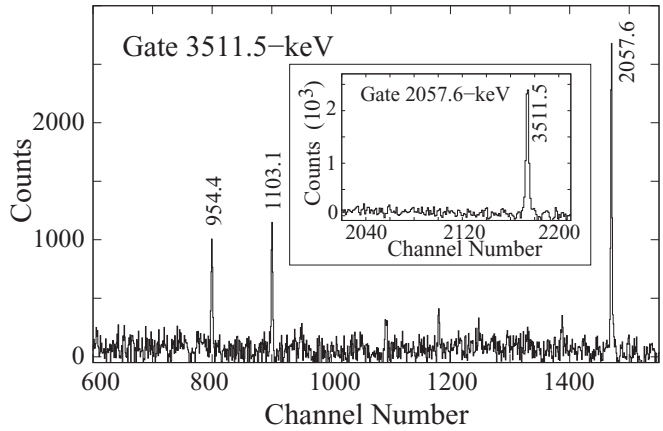

FIG. 11. γ spectrum gated on the 3511.7-keV line corresponding to the primary transition from the ^{96}Zr$(n,\gamma)^{97}$Zr reaction. The inset shows γ spectrum gated on the 2057.6-keV line. Lines are labeled with their γ energies.

triple-γ histograms, and by gating on the known sums in cascades of ^{97}Zr in the $gS2$ histogram.

The construction of the level scheme started with the analysis of the γ spectrum coincident with the 1103.3-keV $3/2^+ \rightarrow 1/2^+$ transition in ^{97}Zr. After excluding lines belonging to Hf isotopes (coincident with the 1102.8-keV transition of ^{178}Hf [16] and the 161-keV transition of ^{179}Hf [17]) we could identify γ lines belonging to the ^{97}Zr nucleus, including those corresponding to primary transitions. Figure 11 shows, as an example, a spectrum gated on a γ line corresponding to the 3511.7-keV primary transition.

The excitation scheme of ^{97}Zr populated in the (n,γ) reaction, obtained in the present work, is shown in Fig. 12. The newly found transitions are marked with asterisks. In ^{97}Zr we have observed, in total, 57 γ transitions and 23 excited states. Of these, 47 transitions and 14 excited levels are newly identified in (n,γ). The information on the observed γ transitions and excited levels is summarized in Table II. Because of the strong contamination of singles spectra by Hf lines we have estimated intensities of γ lines in ^{97}Zr using coincidence spectra. The resulting values are in relative units, with the intensity of the 4465.8-keV line set to 100.

2. *Results from beta decay of* ^{97}Y

Using the data from the β-decay of ^{97}Y collected at Lohengrin and sorted into multiple-γ histograms we could verify the existing β-decay data [7]. The present measurement provided more precise energies of γ lines and energies of excited levels, than reported before [7]. The values obtained in this work are listed in Table III. Because the decays of the $1/2^-$ ground state and the $9/2^+$ isomer in ^{97}Y could not be separated sufficiently in our measurement, we do not report γ intensities.

The scheme of excitations populated in β decay, as observed in this work is shown in Fig. 13.

Using coincidence data we could confirm transitions of ^{97}Zr reported in Ref. [7], except the 1207.1-, 1219.2-, 1438.9-, 1549.3-, 1617.2-, 1811.9-, and 2943.3-keV decays, which are not seen in our data.

The following transitions reported as uncertain in Ref. [7] are confirmed in this work (we use energies from Table III): 135.6, 274.4, 596.1, 652.3, 767.3, 834.4, 954.1, 962.2, 980.0, 1002.2, 1131.6, 1328.6, 1337.4, 1370.5, 1492.4, 1523.2, 1524.5, 1537.8, 1575.1, 1639.6, 1707.5, 1896.6, 2160.0, and 2311.4 keV. These transitions are confirmed at positions in the level scheme reported in Ref. [7], except the 1492.4-keV transition, which feeds the 2625.6-keV level, not the 2626.6-keV level.

We observe a new 2699.2-keV transition decaying the 3964.0-keV level.

We confirm the following levels in ^{97}Zr reported in Ref. [7] as tentative (we use energies from Table III): 3136.1, 3146.5, 3186.0, 3471.3, and 4148.7 keV. The 1848-, 2813.7-, 3026.1-, and 3402.0-keV levels reported in Ref. [7] could not be confirmed in the present work. We introduce a new 4118.9-keV level, assigning to it the 1854.0- and 2311.4-keV decays, which were attributed to the 4117.8-keV level in Ref. [7].

3. *Other observations*

A surprising fact is the nonobservation in the (n,γ) data of the 3401.2-keV $(3/2^-)$ and the 3549.0-keV $(1/2, 3/2)$ levels, which are observed in the β^- decay of the $1/2^-$ ground state in ^{97}Y. The absence of the 3401.2-keV level is particularly intriguing, because the neighboring 3287.7-keV $(3/2^-)$ level is strongly populated in the (n,γ) reaction. We note that the 3287.7- and 3401.2-keV levels receive the highest population in the β^- decay of the $1/2^-$ ground state in ^{97}Y, with respective log ft values of 4.6 and 4.7, suggesting similar structure of the two levels.

Our search for new excitations of a possible isomeric nature gave negative result over a wide range of half-lives from 0.5 μs to 5 ms. We thus exclude the existence of a low-lying, long-lived $11/2^-$ isomer of a single-particle (s.p.) nature in ^{97}Zr.

B. Spin-parity assignments to levels in ^{97}Zr

The determination of spins and parities of levels in ^{97}Zr is the most important goal of the present work. In this section we present a detailed discussion of this subject and show the obtained results. In the discussion we use γ energies as listed in Tables II and III when referring to the (n,γ) and β-decay measurements, respectively.

The compilation [7] reports firm spins and parities of $1/2^+$ for the ground state and $7/2^+$ for the 103 ns isomer at 1264.7 keV in ^{97}Zr. Starting with these two assignments we worked out spins and parities of other levels in ^{97}Zr based on angular-correlation measurements, using data from the (n,γ) and fission measurements with EXILL as well as the polarization-directional correlations measured with EXILL. The results of the correlations are summarized in Tables IV and V.

Spin-parity assignments in ^{97}Zr were helped by the observed intensities of primary transitions, knowing that decays corresponding to spin change $\Delta I \leqslant 1$ are usually more intense than decays corresponding to $\Delta I > 1$. We also used γ

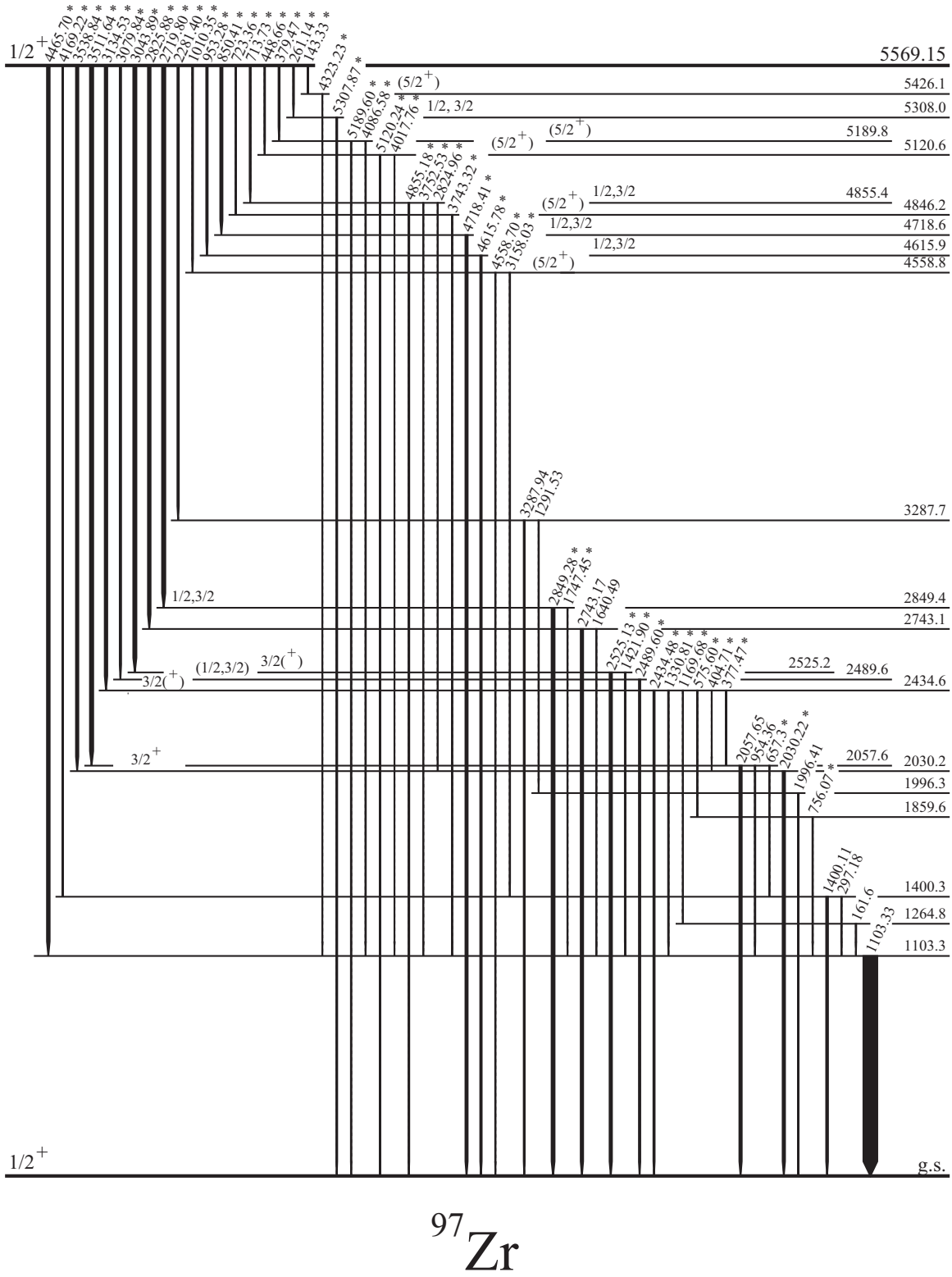

FIG. 12. The excitation scheme of ^{97}Zr populated in (n, γ) as observed in the present work. The newly found γ transitions are marked with asterisks. Spins are shown for excited levels populated exclusively in (n, γ). Spins of other levels are shown in Fig. 13.

TABLE II. Excitation energies E_{exc}, γ-line energies E_γ, and relative γ intensities I_γ in ^{97}Zr, as obtained from the (n,γ) measurement performed in the present work.

Secondary γ transitions			Primary γ transitions		
E_{exc} (keV)	E_γ (keV)	I_γ (rel.)	E_{exc} (keV)	E_γ (keV)	I_γ (rel.)
1103.3	1103.33(5)	$\geqslant$509(20)	5569.15	143.33(30)	$\geqslant$5(2)
1264.8	161.6(3)	23(2)		261.14(7)	$\geqslant$35(6)
1400.3	297.18(8)	22(2)		379.47(15)	$\geqslant$40(5)
	1400.11(18)	68(5)		448.66(7)	$\geqslant$28(4)
1859.6	756.07(9)	17(2)		713.73(5)	$\geqslant$42(5)
1996.3	1996.41(15)	$\geqslant$15(2)		723.36(32)	$\geqslant$12(2)
2030.2	2030.22(5)	88(4)		850.41(5)	$\geqslant$82(5)
2057.6	657.3(3)	7(1)		953.28(5)	$\geqslant$54(4)
	954.36(15)	25(3)		1010.35(11)	$\geqslant$36(3)
	2057.65(5)	88(6)		2281.40(8)	$\geqslant$53(4)
2434.6	377.47(22)	4(1)		2719.80(5)	$\geqslant$120(16)
	404.71(24)	4(1)		2825.88(6)	$\geqslant$98(9)
	575.60(16)	6(1)		3043.89(8)	$\geqslant$116(7)
	1169.68(25)	8(1)		3079.84(12)	$\geqslant$51(5)
	1330.81(13)	26(2)		3134.53(7)	$\geqslant$94(7)
	2434.48(7)	46(4)		3511.64(6)	$\geqslant$120(10)
2489.5	2489.60(9)	51(5)		3538.84(5)	$\geqslant$88(4)
2525.2	1421.90(20)	28(2)		4169.22(14)	8(2)
	2525.13(7)	88(6)		4465.70(5)	**100(3)**
2743.1	1640.49(31)	8(1)			
	2743.17(8)	90(8)			
2849.4	1747.45(25)	10(3)			
	2849.28(5)	110(15)			
3287.7	1291.53(26)	15(2)			
	3287.94(8)	38(3)			
4558.8	3158.03(40)	20(2)			
	4558.70(20)	16(2)			
4615.9	4615.78(8)	54(4)			
4718.6	4718.41(7)	82(5)			
4846.2	3743.32(30)	12(2)			
4855.4	2824.96(25)	4(1)			
	3752.53(25)	7(1)			
	4855.18(5)	31(3)			
5120.6	4017.76(30)	11(2)			
	5120.24(23)	17(3)			
5189.8	4086.58(21)	18(3)			
	5189.60(28)	22(3)			
5308.0	5307.87(9)	35(7)			
5426.1	4323.23(48)	5(1)			

branchings for excited levels, shown in Table II as well, as arguments from a comparison of populations in the (n,γ) and β-decay reactions. In the assignments we considered log ft values reported in Ref. [7].

Spin-parity assignments to levels in ^{97}Zr, as obtained in this work, are shown in Figs. 12 and13. In the following text we discuss these assignments in detail.

1. 1103.3-keV level and the 1103.3-keV transition

The level at 1103.3 keV is reported with spin-parity $3/2^+$ [7], though it is based on weaker arguments than for the $1/2^+$ ground state or the $7/2^+$ isomer. Angular correlations from EXILL fission are consistent with two spin solutions, 3/2 and 5/2 for the 1103.3-keV level. Using the data from (n,γ) for the 4465.7–1103.3-keV cascade we can reject the 1/2-5/2-1/2 spins in the cascade, for which the theoretical coefficients of $A_2 = 0.29$ and $A_4 = 0.38$ are clearly different from the experimental A_k/A_0 values shown in Table IV. The 3/2 spin assignment is consistent with the high intensity of the 4465.7-keV primary transition.

Positive parity of the 1103.3-keV level is firmly established by the stretched $E2$ multipolarity of the 161.5-keV decay of the $7/2^+$ isomer at 1264.7 keV [7]. With spin 3/2, the mixing ratio δ is $+0.27(4)$ or $-3.8(5)$ for the 1103.3-keV transition. Considering the prompt character of this transition, both solutions indicate its $M1+E2$ multipolarity and a positive parity of the 1103.3-keV level.

The experimental value of linear polarization for the 1103.3-keV transition, $P_{exp} = -0.14(3)$, obtained from the directional-polarization correlation with the 161.5-keV stretched $E2$ transition, helps to determine the mixing ratio. The theoretical linear polarization for $M1+E2$ is $-0.124(2)$ for $\delta = +0.27(4)$ and $+0.124(2)$ for $\delta = -3.8(5)$, clearly indicating $\delta = +0.27(4)$ for the 1103.3-keV transition. This value will be used in the correlation analyses of other transitions.

2. 1400.3- and 3287.7-keV levels

The 3287.7-keV level has a tentative $(3/2^-)$ spin-parity assignment in Ref. [7]. This is based on the log ft of 4.6 for the 3287.7-keV level, which indicates an allowed Gamow-Teller (G-T) transition to this level from the $(1/2^-)$ ground state of ^{97}Y. Angular correlations for the 2281.4–3287.9-keV cascade in the (n,γ) data allow a spin 5/2 to be rejected for the 3287.7-keV level. The 3/2 spin of the 3287.7-keV levels is consistent with the high intensity of the 2281.4-keV primary γ decay.

The 1400.3-keV level has tentative $(3/2^+, 5/2^+)$ spin-parity assignment [7]. With spin 3/2 of the 3287.7-keV level, angular correlations for the 1887.4–1400.3-keV cascade observed in the EXILL-fisison data indicate uniquely spins 3/2-5/2-1/2 in the cascade, with the mixing coefficient $\delta(1887.5) = -0.03(4)$, as shown in Fig. 14. The prompt character the 1400.3-keV transition indicates its stretched $E2$ multipolarity and, consequently, positive parity of the 1400.3-keV level.

The $5/2^+$ assignment to the 1400.3-keV level is consistent with angular correlations for the 297.2–1103.3-keV cascade and with the population of the 1400.3-keV level in the (n,γ) data.

The experimental polarization of the 1887.4-keV transition of $+0.56(40)$ from the 1887.4–1400.1-keV cascade is consistent with an $E1$ multipolarity for the 1887.4-keV transition. This indicates negative parity for the 3287.7-keV level because the theoretical polarization at $\delta(1887.4) = -0.03(4)$ is $+0.29(2)$ for an $E1+M2$ multipolarity and $-0.29(2)$ for an $M1+E2$ multipolarity.

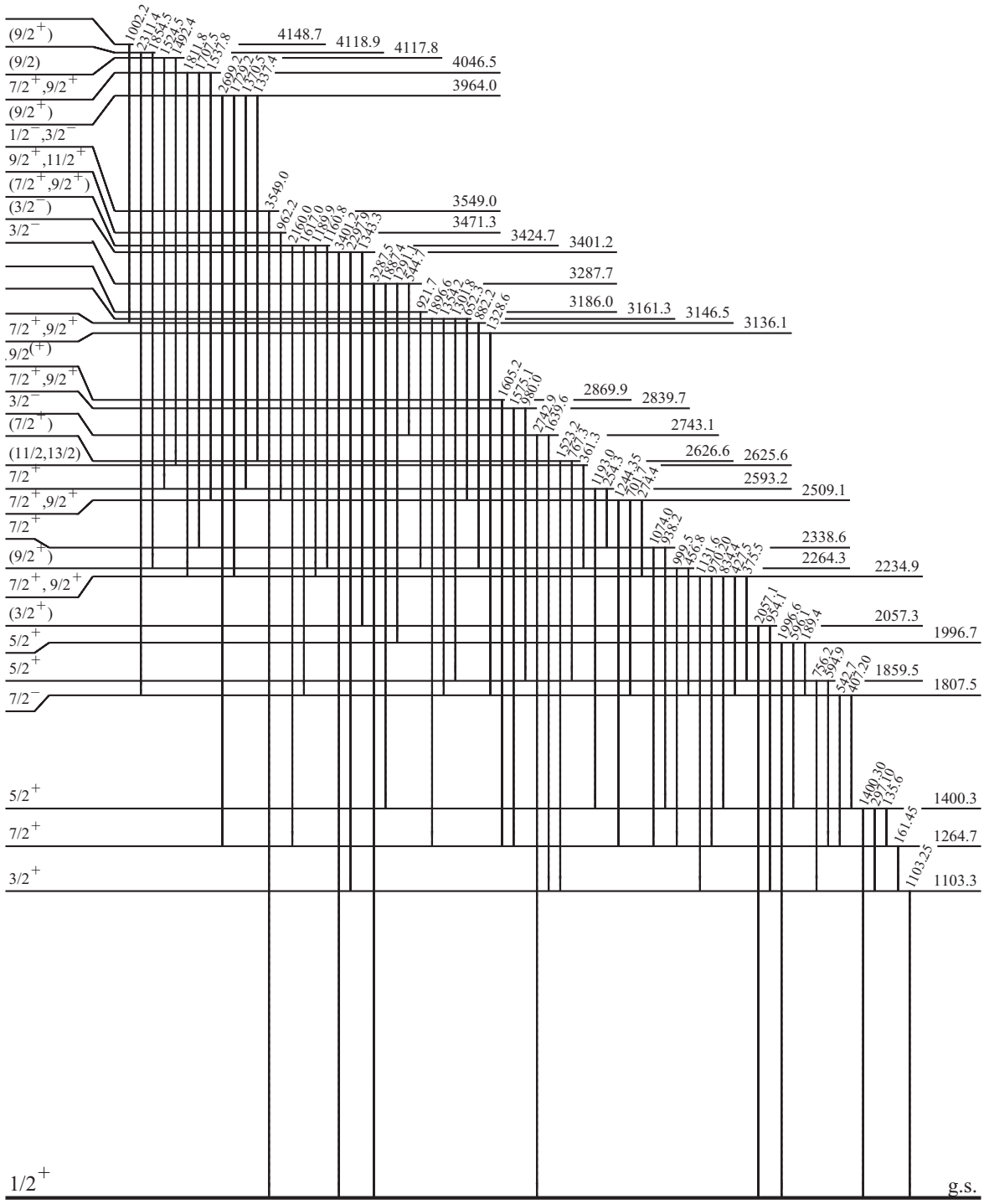

^{97}Zr

FIG. 13. Scheme of excited levels in ^{97}Zr populated in β decay of ^{97}Y, as observed in the present work.

3. 1807.5-keV level

The spin-parity of the 1807.5-keV level reported in Ref. [7] is $(7/2^-)$. This level is clearly observed in the β^- decay of the $9/2^+$ isomer of ^{97}Y but not seen in our (n,γ) data, which suggests a spin higher than $5/2$. This is also suggested by the decay branching of the 1807.5-keV level.

TABLE III. Energies of excited levels and γ lines in ^{97}Zr as obtained in this work from β decay of ^{97}Y measurement at Lohengrin.

E_i (keV)	E_γ (keV)	E_i (keV)	E_γ (keV)
1103.3	1103.25(5)	2869.9	1605.2(2)
1264.7	161.45(5)	3136.1	1328.6(1)
1400.3	135.6(2)	3146.5	882.2(2)
	297.10(5)	3161.3	652.3(3)
	1400.30(5)		1301.8(1)
1807.5	407.20(5)		1354.2(3)
	542.7(1)		1896.6(1)
1859.5	594.9(1)	3186.0	921.7(1)
	756.2(1)	3287.7	544.7(1)
1996.7	189.4(2)		1291.1(1)
	596.1(1)		1887.4(1)
	1996.6(1)		3287.5(2)
2057.3	954.1(3)	3401.2	1343.3(3)
	2057.1(3)		2297.9(3)
2234.9	375.5(1)		3401.2(2)
	427.5(1)	3424.7	1160.8(3)
	834.4(2)		1189.9(2)
	970.20(5)		1617.0(3)
	1131.6(1)		2160.0(2)
2264.3	456.8(1)	3471.3	962.2(2)
	999.5(1)	3549.0	3549.0(2)
2338.6	938.2(1)	3964.0	1337.4(2)
	1074.0(1)		1370.5(2)
2509.1	274.4(2)		1729.2(2)
	701.7(1)		2699.2(3)
	1244.35(5)	4046.5	1537.8(4)
2593.2	254.3(2)		1707.5(4)
	1193.0(1)		1811.8(3)
2625.6	361.3(1)	4117.8	1492.4(2)
2626.6	767.3(3)		1524.5(3)
	1523.2(1)	4118.9	1854.5(2)
2743.1	1639.6(2)		2311.4(2)
	2742.9(1)	4148.7	1002.2(2)
2839.7	980.0(2)		
	1575.1(1)		

With spin-parity $5/2^+$ of the 1400.3-keV level, determined above, angular correlations for the 407.2–1400.3-keV cascade in the EXILL data exclude spins $1/2$ and $9/2$ for the 1807.5-keV level. The correlations fit very well spin $7/2$ for the 1807.5-keV level with $\delta(407.2) = 0.00(2)$, which is consistent with an $E1$ multipolarity for the 407.2-keV transition and negative parity for the 1807.5-keV level. Experimental linear polarization of +0.17(12) for the 407.2-keV transition indicates an $E1$ multipolarity [the theoretical value at $\delta(407.2) = 0.00(2)$ is +0.103(5) for $E1$ and −0.103(5) for $M1$. Negative parity is also supported by the log $ft = 6.3$ for the decay from the $9/2^+$ isomer in ^{97}Y to the1807.5-keV level.

4. 1859.5-keV level

The 1859.5-keV level has a tentative $(3/2^+, 5/2^+)$ spin assignment in [7]. Spin $5/2$ is consistent with low feeding of this level in the decay of the capture level in ^{97}Zr and with log $ft = 6.8$ in the decay of the $1/2^-$ ground state of ^{97}Y [7], which excludes spin $7/2$ for the 1859.5-keV level. The observed β decay of the $9/2^+$ isomer in ^{97}Y to the 1859.5-keV level also favors spin-parity $5/2^+$.

For the $5/2$ spin of the 1859.5-keV level and $3/2^+$ spin of the 1103.1-keV level, angular correlations indicate an $M1 + E2$ multipolarity of the 756.2-keV transition with $\delta(756.2) = -1.3(9)$, thus positive parity of the 1859.5-keV level. The polarization for the 756.2-keV transition is consistent with spin-parity $5/2^+$ rather than spin-parity $3/2^+$ reported for this level in Ref. [30].

5. 1996.7-keV level

The 1996.7-keV level has a tentative $(5/2^+)$ spin assignment in [7]. With spin $3/2$ of the 3287.7-keV level, angular correlations for the 1291.1–1996.6-keV cascade in the EXILL data, shown in Fig. 10, provide unique spin $5/2$ for the 1996.7-keV level with mixing ratio $\delta(1291.1) = 0.010(16)$.

With spin $5/2$ of the 1996.7-keV level the experimental polarization for the 1291.1-keV transition of +0.25(17) indicates its $E1 + M2$ multipolarity because the theoretical polarization at $\delta = 0.01(2)$ is +0.270(5). Considering the negative parity of the 3287.7-keV level, the parity of the 1996.7-keV level is positive. This is consistent with the prompt character of the 1996.6-keV stretched-$E2$ decay.

6. 2057.3-keV level

The 2057.3-keV level has a tentative $(5/2^+)$ spin assignment in Ref. [7], which is a compromise between the (d, p) measurement pointing to spin-parity $(3/2^+, 5/2^+)$ and the β-decay measurement suggesting spins $(7/2, 9/2, 11/2)$ [7].

The 2057.3-keV level is strongly populated in the decay of the capture level in the (n, γ), which suggests spin $1/2$ or $3/2$ for this level. Angular correlations for the 3511.7–2057.7-keV cascade in the (n, γ) data reject spin $1/2$ for this level and are consistent with spin $3/2$ or $5/2$. Therefore, we propose spin $3/2$ for the 2057.3-keV level. Positive parity is more likely, considering low population of this level in β decay of the $1/2^-$ ground state of ^{97}Y.

It should be noted, though, that spin $3/2^+$ is inconsistent with the log $ft = 6.2$ for the 2057.3-keV level reported in β decay of the $9/2^+$ isomer in ^{97}Y [7].

7. 2234.9-keV level

The 2234.9-keV level has a tentative $(7/2^+)$ spin assignment in [7] based on the log $ft = 4.6$ observed in the decay of the $9/2^+$ isomer in ^{97}Y. It is not populated in the decay of the capture level in our (n, γ) data, which is consistent with spin higher than $5/2$.

Angular correlation for the 970.2–161.5-keV cascade observed in the EXILL data fits well with spin $7/2$ for the 2234.9-keV level with $\delta(970.0) = 0.71(4)$, as shown in Fig. 15. This indicates an $M1 + E2$ multipolarity for the prompt 970.2-keV transition, thus positive parity for the 2234.9-keV level.

Experimental linear polarization for the 970.0-keV transition is −0.11(6) while the theoretical value in the 7/2-7/2-3/2 cascade at $\delta(970.0) = 0.71(4)$ is +0.250(2) for an

TABLE IV. Experimental angular-correlation coefficients A_k/A_0 and the corresponding mixing ratios δ for γ transitions in γ-γ cascades of ^{97}Zr, determined for various spin hypotheses. The correlations were observed (a) following neutron-induced fission of ^{235}U measured with EXILL, and (b) following the (n, γ) reaction measured with EXILL.

Cascade γ_1-γ_2	A_2/A_0 (exp.)	A_4/A_0 (exp.)	I_1-I_2-I_3 δ_{γ_2}	δ_{γ_1}
(a) ^{235}U + n				
970.2–161.5	− 0.072(11)	0.045(23)	7/2-7/2-3/2 $\delta_{\gamma_2} = 0$	0.71(4)
999.5–161.5	− 0.016(20)	− 0.059(41)	9/2-7/2-3/2 $\delta_{\gamma_2} = 0$	4.3(6)
1244.4–161.5	0.083(44)	− 0.076(101)		
1605.2–161.5	− 0.31(8)	0.06(15)	9/2-7/2-3/2 $\delta_{\gamma_2} = 0$	− 0.38(15) or –3.6(15)
161.5–1103.3	− 0.004(7)	− 0.018(20)	7/2-3/2-1/2 $\delta_{\gamma_2} = 0.27(4)$ or -3.8(5)	0
756.2–1103.3	− 0.050(21)	− 0.011(46)	5/2-3/2-1/2 $\delta_{\gamma_2} = 0.27$	− 1.3(9)
407.2–1400.3	− 0.071(14)	0.026(29)	7/2-5/2-1/2 $\delta_{\gamma_2} = 0$	− 0.00(2)
938.2–1400.3	− 0.52(9)	0.03(15)	7/2-5/2-1/2 $\delta_{\gamma_2} = 0$	1.0(5)
1193.0–1400.3	0.233(54)	0.076(126)	7/2-5/2-1/2 $\delta_{\gamma_2} = 0$	0.8(4)
1887.4–1400.3	− 0.167(41)	0.039(87)	3/2-5/2-1/2 $\delta_{\gamma_2} = 0$	− 0.03(4)
1291.1–1996.6	− 0.211(15)	− 0.014(30)	3/2-5/2-1/2 $\delta_{\gamma_2} = 0$	0.01(2)
1343.3–2057.6	0.104(76)	− 0.034(160)		
544.7–2743.1	− 0.150(26)	− 0.012(60)		
(b) ^{96}Zr$(n, \gamma)^{97}$Zr				
297.2–1103.3	− 0.20(12)	− 0.01(28)	5/2-3/2-1/2 $\delta_{\gamma_2} = 0.27$	0.8(50)
4465.7–1103.3	0.012(48)	− 0.084(107)	1/2-3/2-1/2 $\delta_{\gamma_2} = 0.27$	− 3.2(9)
3511.7–2057.7	0.314(70)	0.120(150)		
3134.5–2434.6	− 0.317(86)	− 0.211(164)		
2825.9–2743.1	0.169(46)	0.051(100)		
2281.4–3287.9	− 0.060(85)	− 0.054(197)		
2719–2849.6	− 0.051(48)	0.089(99)		

$M1 + E2$ multipolarity, which is in conflict with the positive parity of the 2234.9-keV level.

The assumption of 9/2-7/2-3/2 spins in the cascade provides worse fit in the angular-correlation analysis ($\chi^2 \approx 4$) but the theoretical linear polarization for the resulting $\delta = 0.0$ is -0.103 for an $M1 + E2$, in good agreement with the experimental polarization.

We note that the above inconsistency may originate from the 103 ns half-life of the 1264.7-keV level [7]. Such a half-life may influence the spin alignment in the intermediate level in the cascade, reducing experimental anisotropies.

We have checked that a moderate increase by 15% of the anisotropy in the 970.0–161.2-keV cascade in ^{97}Zr would improve the angular-correlation fit for 9/2-7/2-3/2 spins and worsen the fit for 7/2-7/2-3/2 spins in the cascade, while not changing significantly δ values and theoretical polarizations.

Concluding, the $9/2^+$ spin-parity assignment for the 2234.9-keV level is preferred, though spin $7/2^+$ cannot be excluded.

8. 2264.3-keV level

The 2264.3-keV level has a tentative $(11/2^-)$ spin assignment in the compilation [7], which follows a suggestion of Ref. [6]. The $\log ft = 6.1$ in a decay of the $9/2^+$ isomer in ^{97}Y to this level allows spins (7/2, 9/2, 11/2) [7].

The angular correlation for the 999.5–161.5-keV cascade obtained from the EXILL data, which is nearly isotropic, is not consistent with spins 11/2-7/2-3/2 in this cascade.

TABLE V. Experimental, $P_{\exp}(\gamma^p)$, and calculated, $P_{th}(\gamma^p)$, values of linear polarization for γ^p transitions in ^{97}Zr observed in this work. The experimental data are from directional-polarization correlations for γ-γ cascades in ^{97}Zr, measured following the neutron-induced fission of ^{235}U using EXILL.

Cascade $\gamma \rightarrow \gamma$	$P_{\exp}(\gamma^p)$	Spins in cascade	Multipol. of γ^p	$P_{th}(\gamma^p)$
161.5–1103.3^p	−0.14(3)	7/2-3/2-1/2	$M1+E2$	
			$\delta = 0.27$	−0.124(2)
			$\delta = -3.8$	+0.124(2)
999.5^p–161.5	−0.21(15)	9/2-7/2-3/2	$M1+E2$	
			$\delta = 4.3$	−0.326(5)
756.2–1103.3^p	0.19(19)	5/2-3/2-1/2	$M1+E2$	
			$\delta = 0.27$	0.000(1)
407.2^p–1400.3	0.17(12)	7/2-5/2-1/2	$E1+M2$	
			$\delta = 0.00$	0.103(5)
1887.4^p–1400.3	0.56(40)	3/2-5/2-1/2	$E1+M2$	
			$\delta = -0.03$	0.29(2)
1291.1^p–1996.6	0.25(15)	3/2-5/2-1/2	$E1+M2$	
			$\delta = 0.01$	0.270(5)
970.2^p–161.5	−0.11(6)	7/2-7/2-3/2	$E1+M2$	
			$\delta = 0.71$	0.250(2)
544.7^p–2743.1	−0.44(22)			

For spins 7/2-7/2-3/2 there is no acceptable solution. For the 9/2-7/2-3/2 spin hypothesis, the correlations provide a good solution with $\delta(999.5) = 4.3(6)$. This result suggests spin-parity $9/2^+$ for the 2264.3-keV level. Theoretical linear polarization at $\delta(999.5) = 4.3(6)$ is −0.326(5) for an $M1+E2$ transition in the 9/2-7/2-3/2 cascade, which agrees with the experimental value of −0.21(15), thus supporting positive parity. Therefore, we propose spin $9/2^+$ for the 2264.3-keV level.

A word of caution is needed because angular correlations of the 999.4-keV decay, reported as an $M2$ in Ref. [6], with the 161.2-keV stretched $E2$ below in the cascade, may be attenuated by the 103 ns half-life of the $7/2^+$ 1264.7-keV intermediate level. However, as discussed in the previous section, this attenuation is probably not large. Furthermore we have checked the presence of such an effect in the same EXILL-fission data for the cascade going across the 163 ns isomer in ^{134}Te [31]. For the 2866.2–1279.0-keV cascade of two stretched quadrupole transitions (comprising also two unobserved intermediate, 115.1- and 297.0-keV, stretched quadrupole transitions) the expected angular correlations are $A_2^{th} = 0.102$ and $A_2^{th} = 0.009$, while the experimental values in the EXILL data are $A_2^{exp} = 0.12(3)$ and $A_2^{exp} = -0.05(6)$, showing that the 163 ns isomer does not attenuate the correlations in ^{134}Te.

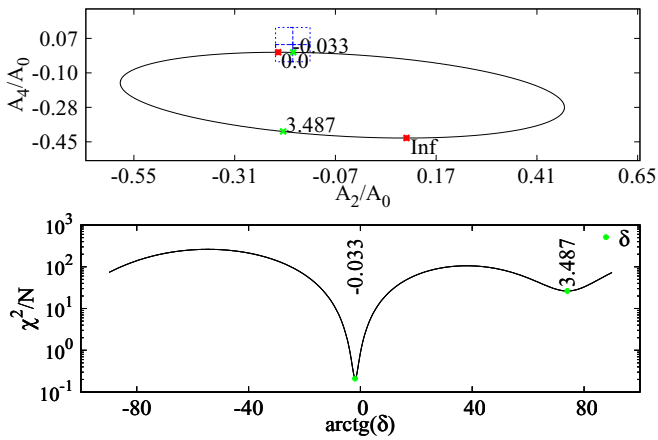

FIG. 14. Angular correlations for the 3/2-5/2-1/2 spin hypothesis in the 1887.4–1400.3-keV cascade as observed in the EXILL fission measurement.

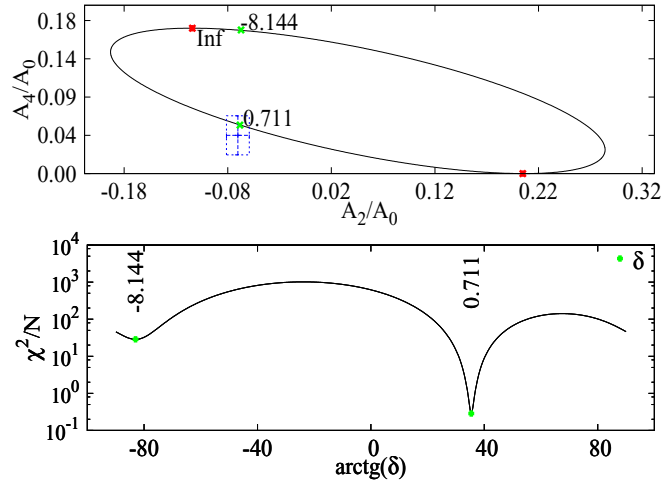

FIG. 15. Angular correlations for the 7/2-7/2-3/2 spin hypothesis in the 970.0–161.2-keV cascade, as observed in the EXILL fission measurement.

9. 2743.1-keV level

The 2743.1-keV level has a tentative (1/2, 3/2) spin assignment in [7]. Spin 5/2 would be inconsistent with the strong feeding by the 4169.2-keV primary decay in the (n,γ) data. Angular correlations in the 2825.9–2743.2-keV cascade from (n,γ) are also inconsistent with the 5/2 spin, while the nonzero anisotropy allows us to reject a spin of 1/2 for the 2743.1-keV level.

Angular correlations for the 544.7–2742.9-keV cascade in the EXILL data are anisotropic, which again rejects spin 1/2 for the 2743.1-keV level. Further analysis needs assumptions. With a positive parity of the 2743.1-keV level, the 544.7-keV transition should be an $E1$ with negligible $M2$ admixture. Assuming $\delta(544.7) = 0$, one obtains from angular correlations $\delta(2742.9)$ of 0.06(4) or −2.0(2) in the 3/2-3/2-1/2 cascade. The experimental polarization of the 544.7-keV transition is −0.44(22), while the theoretical value at $\delta(544.7) = 0$ is −0.22(3) for $M1+E2$ at both values of $\delta(2742.9)$. This is inconsistent with the assumption of an $E1$ multipolarity of the 544.7-keV transition and positive parity for the 2743.1-keV level.

On the other hand, there are many solutions with a nonzero δ ($M1/E2$) of 544.7- and 2742.9-keV transitions, giving

large, negative polarization. Therefore, we propose negative parity for the 2743.1-keV level. The log $ft = 5.47$ for the 2743.1-keV level, populated in the decay of the $1/2^-$ ground state of ^{97}Y, is consistent with the $3/2^-$ spin-parity of this level.

10. 3401.2-keV level

In contrast to the $3/2^-$ 3282.7-keV level, the 3401.2-keV level is not populated in the decay of the neutron-capture level, which might suggest spin higher than 3/2. Angular correlations for the 2057.1–1343.4-keV cascade are consistent with spin 3/2 or 5/2 for the 3401.2-keV level. However, the log $ft = 4.8$ value for this level [7] indicates an allowed Gamow-Teller transition from the $(1/2^-)$ ground state of ^{97}Y, pointing to spin-parity $3/2^-$, as tentatively reported in [7].

11. Other levels

There are clear differences in the populations of levels in the (n, γ) and β-decay reactions, which allow conclusions to be made about their spins.

(i) Levels with spins 1/2, 3/2, or 5/2. In the (n, γ) reaction we observe new levels at 2030.2, 2434.6, 2489.5, 2525.2, 2849.5, 4558.9, 4615.9, 4718.6, 4846.2, 4855.4, 5120.6, 5189.8, 5308.0, and 5426.1 keV, which are not populated in β^- decay of ^{97}Y. These excitations have spins 1/2, 3/2, or 5/2.

The population in the (n, γ) suggests spin 1/2 or 3/2 for the 2434.6- and 2849.4-keV levels. Angular correlations from the (n, γ) data allow us to reject spin 1/2 and 5/2 for the 2434.6-keV level. The prompt 1169.7-keV decay to the $7/2^+$ level at 1264.9 keV suggests positive parity for the 2434.6-keV level.

Angular correlations for the 2719.8–2849.3-keV cascade in the (n, γ) data reject spin 5/2 for the 2849.4-keV level. Negative parity of this level is less likely, because it is not populated in β decay of the $1/2^-$ ground state of ^{97}Y.

The 3549.0-keV level is strongly populated in β decay of the $1/2^-$ ground state of ^{97}Y. It is not populated in (n, γ), similar to the 3401.2-keV level with spin-parity $(3/2^-)$. Both levels decay predominantly to the ground state. Considering the log $ft = 5.4$ of the 3549.0-keV level [7], we propose spin-parity $1/2^-$ or $3/2^-$ for this level.

For other levels of this section we propose spins as shown in Figs. 12 and 13, taking into account branchings of these levels and intensities of primary transitions populating these levels, as shown in Table II.

(ii) Levels with spin higher than 5/2. Several levels reported in β^- decay of the $9/2^+$ isomer in ^{97}Y are not seen in the (n, γ) data. Therefore their spins are probably higher than 5/2. The 1807.5-, 2234.9-, and 2264.3-keV levels of this lot were discussed in previous sections. Other levels are discussed below.

Angular correlations for the 938.2–1400.3-keV cascades clearly reject spins 5/2 and 9/2 for the 2338.6-keV level. For the 7/2 spin there is a solution with $\delta(938.2) = 1.0(5)$, which indicates an $M1 + E2$ character of this transition and positive parity for the 2338.6-keV level. Spin-parity $7/2^+$ is consistent with log $ft = 5.9$ in the decay of the $9/2^+$ isomer in ^{97}Y [7].

Angular correlations for the 1244.4–161.2-keV cascade are consistent with spin 7/2 or 9/2 for the 2509.1-keV level. The log $ft = 5.3$ of this level, reported in decay of the $9/2^+$ isomer in ^{97}Y [7], indicates its positive parity.

Angular correlations for the 1193.0–1400.3-keV cascade are consistent with spin 7/2 for the 2593.2-keV level but not with spin 9/2. Large $\delta(1193.0)$ favors positive parity for this level.

The 2625.6-keV level reported with a tentative $(13/2^-)$ spin-parity [6,29] has no spin assignment in Ref. [7]. The 361.3-keV decay from this level to the $(9/2^+)$ level at 2234.9 keV is seen in our β-decay data, but higher-lying transitions in the cascade populated by the decay of the $(27/2^-)$ 142 ms isomer in ^{97}Y [29] are not observed. Therefore, we conclude that the 2625.6-keV level is populated in the decay of the $9/2^+$ isomer in ^{97}Y. Because it belongs to the cascade populated in decay of the 142 ms isomer, its spin should be higher than 9/2 (we note that it does not decay to 7/2 levels). For this level we propose tentative spin-parity (11/2, 13/2).

The 2626.6-keV level has a tentative $(7/2^+)$ spin-parity in [7]. The 1523.2-keV decay to the $3/2^+$ level at 1103.1-keV excludes spin 9/2. The nonobservation of this level in (n, γ) is consistent with spin higher than 5/2.

We tentatively assign spin $(7/2^+, 9/2^+)$ to the 2839.7-keV level. Spin $11/2^+$ proposed in [7] is very unlikely because of the 980.0-keV decay to the $5/2^+$ level at 1859.5-keV.

For the 2869.9-keV level we propose spin $9/2^{(+)}$. It decays solely to the $7/2^+$ isomer at 1264.7 keV. Angular correlations for the 1605.2–161.5-keV cascade are consistent with spins 9/2-7/2-3/2 only. Large values of δ ratios of the 1605.2-keV favor its $M1 + E2$ multipolarity.

For the 3424.7-keV level, spin-parity $7/2^+$ or $9/2^+$ is proposed based on the observed branchings. The $7/2^-$ spin-parity reported in Ref. [7] is unlikely considering log $ft = 5.3$ for this level. For the same reason spin-parity $11/2^+$ is less likely.

Considering the observed decay of the 3471.3-keV level (3469.9-keV level in [7]), we propose spin-parity $9/2^+$ or $11/2^+$ for this level.

The 3964.0 -keV level decays to a number of $7/2^+$ levels but not to $3/2^+$ or $5/2^+$ levels. Considering its log $ft = 5.5$ [7], we propose tentative spin $9/2^+$ for this level.

The 4046.5-keV level has a tentative $(7/2^+)$ assignment in [7] because of its log $ft = 5.3$. In this work we could not confirm its 2943.3-keV decay to the $3/2^+$ level at 1103.3 keV but we confirm the 1811.8-keV decay to the $7/2^+$ level at 2234.9 keV. We also confirm the 1707.5-keV decay to the $7/2^+$ level at 2338.6 keV level but cannot see any 1538.3-keV decay. Therefore, we propose spin $7/2^+$ or $9/2^+$ for the 4046.5-keV level.

The compilation [7] reports a 4117.8-keV level with log $ft = 5.3$ and tentative $(9/2^+, 11/2^+)$ assignment. In this work we propose two close-lying levels at 4117.8 and 4118.9 keV. The 2311.4-keV decay to the $7/2^-$ level at 1807.5 keV disfavors spin $11/2^+$ for the 4118.9-keV level. Using γ intensities of Ref. [7] we estimate log $ft = 5.4$ for the 4118.9-keV level, which is consistent with spin-parity $9/2^+$ for this level. The estimate for the 4117.8-keV

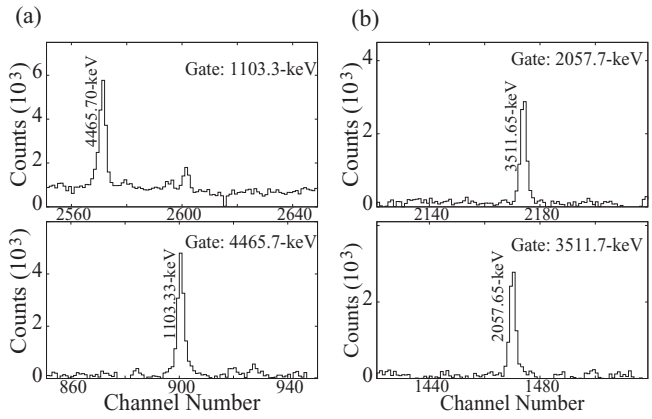

FIG. 16. Coincidence γ spectra gated on (a) the 1103.3- and 4465.7-keV lines and (b) the 2057.7- and 3511.7-keV lines. Lines in spectra are labeled with their γ energies in keV.

level yields $\log ft = 5.9$, which suggests spin $9/2$ for this level.

C. Neutron binding energy of ^{97}Zr

Zr isotopes mark the border between the weak *s* process and the main *s* process [32]. Furthermore, there is a border between the *s* process and the *r* process; ^{96}Zr is considered to be an *r*-process nucleus. It is important to know all details of the structure of these nuclei to improve the existing models of nucleosynthesis of heavier elements. One piece of essential information in this context is the neutron binding energy.

The (n, γ) reaction with cold neutrons populates the neutron-capture level, positioned within millielectronvolts of the neutron binding energy. Therefore the (n, γ) reaction can provide information about neutron binding energy with a precision not available with other techniques. As demonstrated in our previous works [14,33], measurements of γ rays from neutron-capture reactions using arrays of Ge detectors can provide very precise values of neutron-binding energies.

To find the neutron binding energy of the ^{97}Zr nucleus we analyzed $\gamma\gamma$ cascades connecting the capture state with the ground state. Energies of γ transitions were calculated from the energies' γ lines, taking into account the recoil of a nucleus after γ decay. To illustrate the quality of our analysis we show in Fig. 16(a) portion of a γ spectrum gated on the 1103.3-keV line, where one can see a strong 4465.70(5)-keV γ line, corresponding to the 4465.81(5)-keV primary transition and, below, a portion of a γ spectrum gated on the 4465.7-keV γ line, which shows the 1103.33(5)-keV γ line corresponding to the 1103.34(5)-keV transition. From both spectra one can find the sum of the two transition energies of 5569.15(8) keV. Figure 16(b) shows analogous spectra for the 3511.6–2057.7-keV cascade. Energies of transitions in $\gamma\gamma$ cascades deexciting the neutron-capture level are given in Table VI. The new neutron binding energy of 5569.15(4) keV found in this work for ^{97}Zr is calculated as the average value of summed energies in cascades, shown in the third column of the table. In the final uncertainty we included the 0.03-keV systematic error of our energy calibration [11].

TABLE VI. Energies of transitions in twofold cascades deexciting the capture state to the ground state in ^{97}Zr. See text for more information.

E_1 (keV)	E_2 (keV)	$E_1 + E_2$ (keV)
4465.81(5)	1103.34(5)	5569.15(8)
4169.29(14)	1400.12(18)	5569.41(25)
3538.89(5)	2030.24(5)	5569.13(8)
3511.69(7)	2057.67(6)	5569.36(11)
3134.57(7)	2434.50(7)	5569.07(10)
3043.93(8)	2525.16(7)	5569.09(12)
2825.91(6)	2743.10(8)	5569.11(10)
2719.83(5)	2849.32(5)	5569.15(8)
2281.43(8)	3288.00(8)	5569.43(12)
1010.37(11)	4558.81(20)	5569.18(25)
953.20(5)	4615.90(8)	5569.10(10)
850.44(5)	4718.64(7)	5568.98(10)
713.75(5)	4855.32(6)	5569.07(9)
448.67(7)	5120.38(23)	5569.05(24)
379.48(15)	5189.74(28)	5569.22(32)
261.14(7)	5308.02(9)	5569.16(12)

There is a significant difference of 5 keV between the new neutron binding energy of ^{97}Zr and the 5575.1(4)-keV value reported in the compilations [34,35]. To check the correctness of our procedure we have determined neutron binding energies for ^{92}Zr and ^{28}Al isotopes, which are also observed in our experiment. The results of the comparison are shown in Table VII. Our values for ^{92}Zr and ^{28}Al fit very well neutron binding energies reported in the literature [34,35].

IV. DISCUSSION

A. Collectivity in ^{97}Zr

The presence of the collectivity in ^{97}Zr, suggested in [6], is supported by our (n, γ) results, where certain excited levels between 2 and 3 MeV are strongly populated in decays of a complex neutron-capture level, whereas they are not populated following β decay of the $1/2^-$ ground state of ^{97}Y, which has a simpler structure. This observation suggests a collective nature of the 2057.3-, 2434.6-, 2525.2-, 2743.1-, and 2849.4-keV level, identified in this work as $3/2^+$ excitations in ^{97}Zr

The decay of the $9/2^+$ isomer in ^{97}Y populates many levels in ^{97}Zr with spin $7/2^+$. We have identified four $7/2^+$ levels in ^{97}Zr and a few further candidates. In ^{97}Zr the Fermi surface is

TABLE VII. Neutron binding energies for Zr isotopes and ^{28}Al, as obtained in this work. Only statistical error is shown for the present ^{92}Zr and ^{28}Al values.

Isotope	This work	Literature values [34,35]
^{92}Zr	8634.75(4)	8634.79(11)
^{97}Zr	5569.15(4)	5575.1(4)
^{28}Al	7725.174(11)	7725.178(4)

expected near the $g_{7/2}$ neutron orbital. A rather low $\log ft \sim 5$ for these $7/2^+$ levels suggest that they are populated by the allowed $\nu g_{7/2} \rightarrow \pi g_{9/2}$ Gamow-Teller transition. Still, for a final $\nu g_{7/2}$ state with well defined s.p. nature one would expect $\log ft \sim 4$. Therefore, we conclude that the observed $7/2^+$ states in ^{97}Zr with the dominating $(\pi g_{9/2})^2_{0^+} \nu g_{7/2}$ configuration are not of pure s.p. nature. The collectivity present in ^{97}Zr couples to the $\nu g_{7/2}$ s.p. level, causing fragmentation of its strength over several $7/2^+$ excitations. The likely source of this collectivity is the pair of $g_{9/2}$ protons. We note the presence of four 0^+ levels in both ^{96}Zr and ^{98}Zr cores. Coupling of these levels to the $g_{7/2}$ neutron could produce multiple $7/2^+$ levels in ^{97}Zr.

In contrast, one observes few $3/2^-$ levels in ^{97}Zr, of which the 2743.1- and 3287.7-keV levels are firmly identified in this work. The single-particle character is better defined for these $3/2^-$ levels, populated by the $\nu g_{7/2} \rightarrow \pi g_{9/2}$ Gamow-Teller decay of the $1/2^-$ ground state of ^{97}Y containing an admixture of $(\nu g_{7/2})^2$ pair of neutrons. Their $\log ft$ values are lower by 0.5, on average, than the $\log ft$ values of $7/2^+$ levels. This is consistent with the less collective nature of their $[\pi p_{1/2}, (\pi g_{9/2} \nu g_{7/2})_{1^+}]_{3/2^-}$ dominating configuration.

B. New interpretation of the 2264.3-keV level in ^{97}Zr

Considering the discussion above, one might expect a few $11/2^-$ levels in ^{97}Zr of a $(\pi g_{9/2})^2_{0^+} \nu h_{11/2}$ dominating structure, populated in the first-forbidden $\nu h_{11/2} \rightarrow \pi g_{9/2}$ transition. This is not observed.

There are also other doubts about the $\nu h_{11/2}$ single-particle nature of the 2264.3-keV level. In a recent study of octupole excitations in Zr isotopes [36] it was argued that low-lying $11/2^-$ levels in odd-A Zr isotopes are due to octupole excitations rather than to s.p. $\nu h_{11/2}$ excitation. We note that octupole collectivity in ^{97}Zr was already reported in Ref. [6], where the $7/2^-$ level at 1806.6 keV was interpreted as due to an octupole excitation on the $1/2^+$ ground state. Furthermore, the effective s.p. energy extracted in Ref. [36] for the $\nu h_{11/2}$ level shows a significant increase in ^{97}Zr, as compared to lighter Zr isotopes. Such an increase was also suggested in another study [37]. As shown in Ref. [36], the trend for Mo isotopes is significantly different. Therefore, the observation of the $11/2^-$ level at low energy in ^{99}Mo should not be used as an argument supporting the $11/2^-$ spin assignment to the 2264.3-keV level in ^{97}Zr.

One might argue that the unusually high $M2$ rate reported in [6,7] for the 999.5 keV decay is due to the admixture of octupole collectivity in the $11/2^-$ 2264.3-keV level. However in this case the 456.8-keV $E2$ decay of the $7/2^-$ level at 1807.5 keV, suggested to be due to octupole excitation [6], should be orders of magnitude faster than observed.

The above remarks and the angular-correlation result for the 999.5–161.5-keV cascade in ^{97}Zr, obtained in the present work, together with the unusual branching ratio of the 999.5-keV $M2$ and the 456.8-keV $E2$ decays from the 2264.3-keV level reported in [6], raise a question about the $11/2^-$ spin-parity proposed for this level [6,7].

Any other spin-parity assignment and the associated interpretation for the 2264.3-keV level should, first of all, account for its isomeric nature. Three $9/2^+$ isomers, interpreted as due to the $9/2^+[404]$ neutron extruder, were observed in ^{97}Sr, ^{99}Zr, and ^{101}Zr, weakly deformed nuclei [4,8,9,38] at an excitation of about 1 MeV. Therefore, an isomer of this nature may be also present in ^{97}Zr.

We note, that, analogously to $7/2^+$ excitations, there are several $9/2^+$ levels in ^{97}Zr with appreciable population in the β decay of the $9/2^+$ isomer in ^{97}Y. As in the case of the $7/2^+$ level, the $9/2^+$ levels are scattered over a 1.5 MeV energy range and are located about 1.5 MeV above the $7/2^+$ bunch. The $\log ft$ values of the $9/2^+$ level are about 5.5 [7], on average, suggesting retarded Gamow-Teller transitions to these levels. We note that the $\nu g_{7/2} \rightarrow \pi g_{9/2}$ transition, explaining well high population of $7/2^+$ levels in ^{97}Zr in the decay of the $9/2^+$ isomer in ^{97}Y, could not easily explain the high population of several $9/2^+$ levels in ^{97}Zr. Such population can be explained by the $\nu g_{9/2} \rightarrow \pi g_{9/2}$ G-T transition, leading to the $[\nu g_{9/2} (\pi g_{9/2})^2]_{9/2^+}$ dominant configuration. Here, the s.p. strength of the $\nu g_{9/2}$ orbital is fragmented over a number of $9/2^+$ levels by coupling to the collectivity of the cores, as observed for the $7/2^+$ levels.

V. SUMMARY

New low-spin states of ^{97}Zr have been found in the first measurement of γ radiation following cold-neutron capture on a ^{96}Zr target, performed using the highly efficient Ge array EXILL at ILL Grenoble. The measurement provided a new neutron binding energy in ^{97}Zr of 5569.15(4) keV, which is significantly different from the literature value. Angular correlations and directional-polarization measurements obtained from β-decay data provided spin-parity assignments to many levels. We have identified several $7/2^+$ excitations, which are populated in Gamow-Teller β decay of the $g_{7/2}$ neutron present in the wave function of the $9/2^+$ isomer in ^{97}Y. Furthermore, we identified several $9/2^+$ excitations in ^{97}Zr, which are populated in the $\nu g_{9/2} \rightarrow \pi g_{9/2}$ G-T transition from the $9/2^+$ isomer in ^{97}Y, containing the admixture of the $g_{9/2}$ neutron pair in its wave function. In particular, we propose that the 2264.3-keV short-lived isomer in ^{97}Zr may have spin-parity $9/2^+$ rather than $11/2^-$, and may originate from the $\nu g_{9/2}$ rather than from the $\nu h_{11/2}$ orbital. The presence of the $\nu g_{9/2}$ orbit near the Fermi level in ^{97}Y and ^{97}Zr would be consistent with the observation of $9/2^+$ isomers in ^{97}Sr and ^{99}Zr originating from the $\nu g_{9/2}$ extruder orbital.

ACKNOWLEDGMENTS

This work has been partly supported by the Polish National Science Centre under Contract No. DEC-2013/09/B/ST2/03485. The authors thank the technical services of the ILL, LPSC, and GANIL for supporting the EXILL campaign.

[1] T. Werner, J. Dobaczewski, M. W. Guidry, W. Nazarewicz, and J. A. Sheikh, Nucl. Phys. A **578**, 1 (1994).

[2] J. Skalski, S. Mizutori, and W. Nazarewicz, Nucl. Phys. A **617**, 282 (1997).

[3] W. Urban, J. L. Durell, A. G. Smith, W. R. Phillips, M. A. Jones, B. J. Varley, T. Rząca-Urban, I. Ahmad, L. R. Morss, M. Bentaleb, and N. Schultz, Nucl. Phys. A **689**, 605 (2001).

[4] W. Urban, J. A. Pinston, J. Genevey, T. Rząca-Urban, A. Złomaniec, G. Simpson, J. L. Durell, W. R. Phillips, A. G. Smith, B. J. Varley, I. Ahmad, and N. Schulz, Eur. Phys. J. A **22**, 241 (2004).

[5] T. Togashi, Y. Tsunoda, T. Otsuka, and N. Shimizu, Phys. Rev. Lett. **117**, 172502 (2016).

[6] G. Lhersonneau, P. Dendooven, S. Hankonen, A. Honkanen, M. Huhta, R. Julin, S. Juutinen, M. Oinonen, H. Penttilä, A. Savelius, S. Törmänen, J. Äystö, P. A. Butler, J. F. C. Cocks, P. M. Jones, and J. F. Smith, Phys. Rev. C **54**, 1117 (1996).

[7] N. Nica, Nucl. Data Sheets **111**, 525 (2010).

[8] J. K. Hwang, A. V. Ramayya, J. H. Hamilton, D. Fong, C. J. Beyer, P. M. Gore, Y. X. Luo, J. O. Rasmussen *et al.*, Phys. Rev. C **67**, 054304 (2003).

[9] A. Złomaniec, H. Faust, J. Genevey, J. A. Pinston, T. Rząca-Urban, G. S. Simpson, I. Tsekhanovich, and W. Urban, Phys. Rev. C **72**, 067302 (2005).

[10] E. Browne and J. K. Tuli, Nucl. Data Sheets **145**, 25 (2017).

[11] M. Jentschel, A. Blanc, G. de France, U. Koster, S. Leoni, P. Mutti, G. Simpson, T. Soldner, C. Ur, W. Urban *et al.* (EXILL Collaboration), J. Instrum. **12**, 11003 (2017).

[12] F. Azaiez, Nucl. Phys. **A654**, 1003c (1999).

[13] C. Rossi Alvarez, Nucl. Phys. News **3**, 10 (1993).

[14] W. Urban, M. Jentschel, B. Märkisch, Th. Materna, Ch. Bernards, C. Drescher, Ch. Fransen, J. Jolie, U. Köster, P. Mutti, T. Rząca-Urban, and G. S. Simpson, J. Instrum. **8**, P03014 (2013).

[15] F. G. Kondev, Nucl. Data Sheets **98**, 801 (2003).

[16] E. Achterberg, O. A. Capureo, and G. V. Marti, Nucl. Data Sheets **110**, 1473 (2009).

[17] C. M. Baglin, Nucl. Data Sheets **110**, 265 (2009).

[18] H. H. Schmidt, P. Hungerford, H. Daniel, T. von Egidy, S. A. Kerr, R. Brissot, G. Barreau, H. G. Börner, C. Hofmeyr, and K. P. Lieb, Phys. Rev. C. **25**, 2888 (1982).

[19] E. Moll, H. Schrader, G. Siegert, H. Hammers, M. Asghar, J. P. Bocquet, P. Armbruster, H. Ewald, and H. Wollnik, Kerntechnik **19**, 374 (1977).

[20] W. Urban, K. Sieja, G. S. Simpson, H. Faust, T. Rząca-Urban, A. Złomaniec, M. Łukasiewicz, A. G. Smith, J. L. Durell, J. F. Smith, B. J. Varley, F. Nowacki, and I. Ahmad, Phys. Rev. C **79**, 044304 (2009).

[21] M. Rudigier, G. S. Simpson, J. M. Daugas, A. Blazhev, C. Fransen, G. Gey, M. Hackstein, J. Jolie, U. Köster, T. Malkiewicz, T. Materna, M. Pfeiffer, M. Ramdhane, J.-M. Régis, W. Rother, T. Thomas, N. Warr, D. Wilmsen, J. Le Bloas, and N. Pillet, Phys. Rev. C **87**, 064317 (2013).

[22] E. A. McCutchan and A. A. Sonzogni, Nucl. Data Sheets **115**, 135 (2013).

[23] K. S. Krane, R. M. Steffen, and R. M. Wheeler, Nucl. Data Tables **11**, 351 (1973).

[24] *The Electromagnetic Interaction in Nuclear Spectroscopy*, edited by W. D. Hamilton (North-Holland, Amsterdam, 1975).

[25] M. Czerwiński, T. Rząca-Urban, W. Urban, P. Bączyk, K. Sieja, B. N. Nyakó, J. Timar, I. Kuti, T. G. Tornyi, L. Atanasova, A. Blanc, M. Jentschel, P. Mutti, U. Köster, T. Soldner, G. de France, G. S. Simpson, and C. A. Ur, Phys. Rev. C **92**, 014328 (2015).

[26] W. Urban, K. Sieja, T. Materna, M. Czerwiński, T. Rząca-Urban, A. Blanc, M. Jentschel, P. Mutti, U. Köster, T. Soldner, G. de France, G. S. Simpson, C. A. Ur, C. Bernards, C. Fransen, J. Jolie, J.-M. Regis, T. Thomas, and N. Warr, Phys. Rev. C **94**, 044328 (2016).

[27] G. Lhersonneau, D. Weiler, P. Kohl, H. Ohm, K. Sistemich, and R. A. Meyer, Z. Phys. A **323**, 59 (1986).

[28] C. R. Bingham and G. T. Fabin, Phys. Rev. C **7**, 1509 (1973).

[29] M. Matejska-Minda, B. Fornal, R. Broda, M. P. Carpenter, R. V. F. Janssens, W. Krolas, T. Lauritsen, P. F. Mantica, K. Mazurek, T. Pawłat, J. Wrzesiński, and S. Zhu, Phys. Rev. C **80**, 017302 (2009).

[30] J. K. Hwang, A. V. Ramayya, J. H. Hamilton, Y. X. Luo, A. V. Daniel, G. M. Ter-Akopian, J. D. Cole, and S. J. Zhu, Phys. Rev. C **73**, 044316 (2006)

[31] A. A. Sonzogni, Nucl. Data Sheets **103**, 1 (2004).

[32] M. Guttormsen, S. Goriely, A. C. Larsen, A. Görgen, T. W. Hagen, T. Renstrøm, S. Siem, N. U. H. Syed, G. Tagliente, H. K. Toft, H. Utsunomiya, A. V. Voinov, and K. Wikan, Phys. Rev. C. **96**, 024313 (2017).

[33] W. Urban, U. Köster, M. Jentschel, P. Mutti, B. Märkisch, T. Rząca-Urban, Ch. Bernards, Ch. Fransen, J. Jolie, T. Thomas, and G. S. Simpson, Phys. Rev. C **94**, 011302(R) (2016).

[34] M. Wang, G. Audi, A. H. Wapstra, F. G. Kondev, M. MacCormick, X. Xu, and B. Pfeiffer, Chin. Phys. C **36**, 1603 (2014).

[35] G. Audi, Nucl. Phys. A **729**, 337 (2003).

[36] E. T. Gregor, M. Scheck, R. Chapman, L. P. Gaffney, J. Keatings, K. R. Mashtakov, D. O'Donnell, J. F. Smith, P. Spagnoletti, M. Thürauf, V. Werner, and C. Wiesman, Eur. Phys. J. A **53**, 50 (2017).

[37] W. B. Walters, Nucl. Phys. A **688**, 318 (2001).

[38] W. Urban, J. A. Pinston, T. Rząca-Urban, A. Złomaniec, G. Simpson, J. L. Durell, W. R. Phillips, A. G. Smith, B. J. Varley, I. Ahmad, and N. Schulz, Eur. Phys. J. A **16**, 11 (2003).